# Ticking hour glasses: Experimental analysis of intermittent flow

Thierry Le Pennec,[1,2] Knut Jørgen Måløy,[1] Alex Hansen,[3] Madani Ammi,[2]
Daniel Bideau,[2] and Xiao-lun Wu[4]

[1] *Fysisk Institutt Universitetet i Oslo, N-0316 Oslo 3, Norway*
[2] *Groupe Matière Condensée et Matériaux, Université de Rennes 1, F-35042 Rennes Cedex, France*
[3] *Institutt for Fysikk, Norges Tekniske Høgskole, N-7034 Trondheim, Norway*
[4] *Department of Physics and Astronomy, University of Pittsburgh, Pittsburgh, Pennsylvania 15260*

(Received 20 March 1995; revised manuscript received 16 October 1995)

Fluctuations in the flow of sand in an hour glass have been investigated experimentally for the case when the interaction between grains and interstitial air is important. During the active phase of the flow, a plug is formed at the narrowest constriction of the hour glass. The plug is below the free-fall arch defining the lower "edge" of the sand heap in the upper chamber. The low-density region between the plug and the arch defines what we call a "bubble." Early during the active (flow) phase, the position of the bubble is stationary, whereas later, it rises into the bulk of the sand and disappears. The position of the arch thus oscillates with a shorter period than the one associated with the active-inactive phase oscillation.

PACS number(s): 05.40.+j, 46.10.+z, 62.20.−x, 62.40.+i

## I. INTRODUCTION

Granular materials exhibit many flow properties different from what are observed in normal fluids [1–3]. Flow in an hour glass exhibits some of these fascinating behaviors. The simplest flow in an hour glass, which is also the most frequently observed, is the steady pouring of sand from the upper chamber to the lower one, with the mass transfer rate being approximately constant. Several experimental and theoretical studies have focused on this type of flow [4–7] with some progress. The granular flow, in the case when the viscosity of the interstitial fluid is negligible, is well described by what is now known as "hour glass theory" [4]. One of the predictions of this theory is that the mass flow rate is independent of the height of sand in the upper chamber, which is also observed in experiments. This behavior is in contrast to a normal fluid for which the flow rate is proportional to the square root of the height.

In this paper we concentrate on a different flow regime, namely when the flow is intermittent. The intermittency is a result of interactions between interstitial air and the grains being important. The fact that the interstitial fluid may affect the flow of grains has been known for some time in the engineering community [4, 8]. However, very few quantitative measurements [9, 10] have been performed, particularly in the regime where flow becomes intermittent. As first reported by Wu *et al.* [9], the intermittent flow in an hour glass occurs only in a narrow range of parameter space; namely, the particle size is in the range $40< d < 300$ $\mu$m for an hour glass having an orifice of diameter $\sim 1$ mm. For smaller particles ($d < 40$ $\mu$m), there is no flow due to strong intergranular interactions. For larger particles ($d > 300$ $\mu$m), the flow is continuous due to an increased permeability of the sand, preventing the buildup of a sufficiently large pressure gradient to obtain intermittency. When the particle size becomes comparable to the diameter $D$ of the orifice, the flow stops again as a result of the formation of a stable arch just above the orifice.

One of the motivations for this work is the observation that the intermittency seen in an hour glass is intimately related to a spontaneous organization of sand in the vicinity of the orifice. This organization process, resulting from delicate interactions between the sand grains and between the grains and air, is highly nonlinear. When sand flows into the lower chamber a pressure gradient is created between the chambers due to compression of the air in the lower chamber and expansion of the air in the upper chamber. The resulting pressure gradient, which is localized in the vicinity of the orifice, inhibits the sand from further motion. We show that the stabilization of a grain-air interface, leading to intermittency, depends on the creation of a plug in the orifice. This plug, stabilized by the pressure difference between the chambers, leads to the propagation of a low-density zone or a "bubble" in the upward direction, similar to that of a gas bubble in a liquid. Though the close relationship between pressure and flow was recognized in our original paper [9], at that time we did not have a means of probing small pressure differences, which turned out to be only one-thousandth of an atmosphere. To establish on a quantitative level the correlations between the pressure fluctuations and the intermittent sand flow, therefore, provides yet another strong motivation for this research. Using a novel laser light deflection technique [10], strong correlations were not only found for large events, involving flow with a large number of sand grains, but also for a weak pulsatile motion of the free-fall arches during the active (flow) phase. This pulsatile motion has a time scale that turned out to be much shorter than the period of the intermittency.

Recently, attempts have been made to model complex flow patterns in hour glasses. In particular, Manger *et al.* [11] have used computer simulations to investigate the ef-

 

fect of hydrodynamic coupling between the flow of sand and air in small constrictions. Their simulations have captured a number of essential features seen in our experiments, such as the intermittent flow, the formation of low-density "bubbles" in the orifice, and the dependency of the flux on particle size. However, we note that in their simulations the average mass flux depends on the height of the sand heap in contrast to what is observed experimentally. This difference may very well be due to the absence of arching in the simulation, as we noted that the effect of arching is difficult to implement in a computer simulation.

Flow in hour glasses shares a number of features that are common in silos and hoppers, which are of great utility values. As useful paradigms these systems have been studied in the past, and many interesting phenomena have been found [9, 12, 13]. Baxter and Behringer [12] studied different modes of sand flow in a two-dimensional hopper, finding density waves whose formation and propagation direction depend on the detailed geometry and the flow rate. The observed propagation patterns were also found to depend on the roughness of the sand. Observations of $1/f$ noise in a closed hour glass have been reported by Schick and Verveen [13]. In a typical flow pattern in the hour glass, the flow takes place in a conical shaped region going through the pile and the sand slides off from the top in a tiny layer [14, 15]. The detailed structure of the flow, though complicated when the interactions between the gas and the sand are present, is very important for designing durable and efficient silos. On a fundamental level, our system represents an interesting two-fluids model for which the granular flow is strongly coupled to the air flow. Here to find a realistic constitutive equation for sand [16] and to couple such an equation with air flow remains a theoretical challenge.

This paper is organized as follows. Section II contains experimental details, including the sample geometry and preparations. In particular, techniques of differential pressure measurement and electrical conductivity measurement are described. In Sec. III the experimental observations and data analyses are presented. Special emphasis is placed on the local structure and dynamics of sand in the neighborhood of the orifice, as it turns out that many interesting flow features, including intermittency and flow patterns in the bulk sand, are essentially determined by the structure and dynamics in this region.

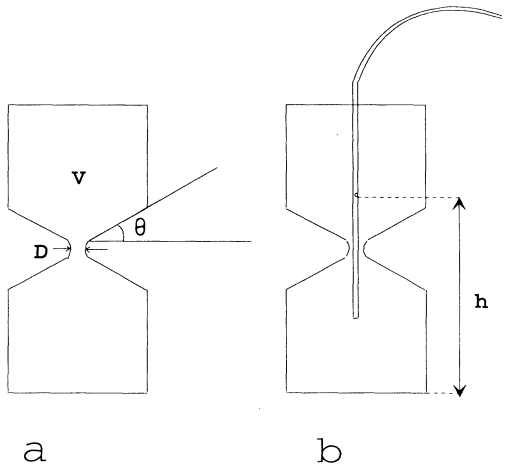


FIG. 1. (a) Drawing of the hour glass to illustrate the geometrical parameters we refer to in the text. (b) The drawing shows the experimental setup for pressure measurements at different heights in the hour glass. A small tube of external diameter 1 mm is introduced into the hour glass. A hole in the tube is introduced at height $h$, where the pressure is measured.

## II. EXPERIMENTAL PROCEDURES

### A. Pressure measurement

Two hour glasses of different volumes $V$ and diameters $D$ of the orifice were used in the experiments. The relevant parameters are defined in Fig. 1. They are given for the hour glass (A): $V = 225$ ml, $\theta = 56°$, and $D = 3.7$ mm, and for the hour glass (B): $V = 409$ ml, $\theta = 65°$, and $D = 2.8$ mm. Glass beads of different diameters, $d = 106 \pm 12$, $89 \pm 22$, $66 \pm 10$, and $55 \pm 10$ $\mu$m, were used. To measure small pressure fluctuations in the hour glasses, we constructed a pressure sensor which is sensitive to a pressure variation down to 0.1 mm of water. The schematic of the setup is shown in Fig. 2. This pressure sensor measures pressure variations with respect to the atmospheric pressure $P_a$. The sensor is connected to the hour glass by a hard plastic tubing which is 15 cm in length. The front end of the sensor is a mirror made of a thin glass plate, 0.1 mm in thickness, coated with aluminum. An input He-Ne laser is split into two beams with the primary beam $i_1$ being reflected from the mirror while the secondary beam $i_2$ serves as an intensity reference. The position of the primary beam is defined by a knife edge, as shown in Fig. 2. A small change in pressure inside the hour glass causes the mirror to bend slightly, thus deflecting the primary laser beam from its unperturbed position. Since $i_1$ is constantly normalized by $i_2$, $i_1/i_2$, the background noise due to either the laser or the photodetectors is significantly reduced. A simple calculation shows that for small pressure fluctuations $\Delta P(\equiv P - P_a)$, $i_1/i_2$ is linearly proportional to $\Delta P$.

The pressure sensor was calibrated by measuring the pressure difference between two containers filled with water. One container was closed except for the tube connec-

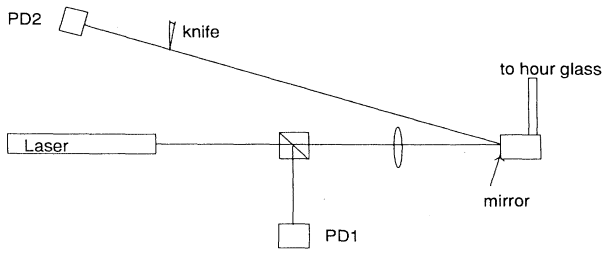


FIG. 2. The experimental setup used in the pressure measurements.

tions to the pressure sensor and to the other container. The second container was open to the atmosphere. Both containers were partially filled with water, and the tube connecting the containers was also filled with water. By varying the height difference between the water levels using a translation stage, we calibrated the pressure sensor in terms of the water height. As expected here a good linear relation between $i_1/i_2$ and $\Delta P(\equiv P - P_a)$ was found.

The pressure measurements were performed in the presence of sand. Here the measurements were carried out in both the lower and the upper chambers, and inside the sand heap with the upper chamber open to the atmosphere. When the pressure was measured in the sand, the sensor was connected to a steel tube with the outer diameter 1 mm and the inner diameter 0.75 mm, as shown in Fig. 1. The tube was closed except for a small hole in the middle where the pressure was sensed. The hour glass was placed on a translation stage so that pressure at different heights inside the sand heap could be measured. To ensure the same perturbation due to the intruding tube for all the measurements, the end of the tube was always in the lower chamber.

### B. Conductance measurement

To have a qualitative assessment of the way that sand packs together near a small constriction we constructed an hour glass similar to (B) with two electrodes (diameter = 2.0 mm) mounted on the opposite sides of the orifice. The diameter of the orifice itself was $D = 2.8$ mm and the electrodes were located at 2 mm above the narrowest region of the orifice, as shown in Fig. 3. The conductance measurements are sensitive to small changes in the granular pressure within the sand and to the movement of the free-fall arch, which will be defined later. A simple calculation [17] suggests that the conductance across the electrodes is proportional to the mean coordination number (i.e., average number of contacts per grain) of the contact network of the sand between the electrodes. Thus, measuring the conductance gives an estimate of the coordination number in the sand heap, which is directly related to the level of compactification and the stability of the heap.

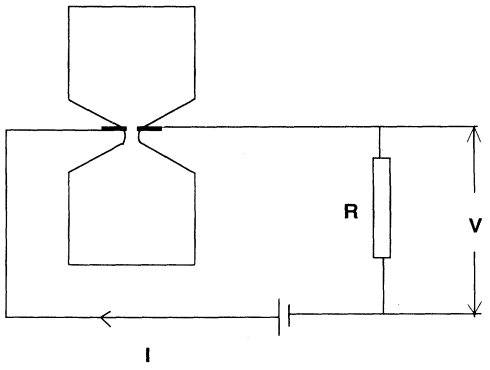


FIG. 3. Experimental setup for conductance measurements. The conductance is measured by observing the voltage drop over the resistance $R$. The current $i$ is about 30 mA and $R = 1.2\ \Omega$. The orifice of the hour glass used in these measurements is $D = 2.8$ mm.

In these experiments we used silver coated glass beads with average diameters $d = 66$ and 89 $\mu$m. To prevent the contact points between the grains from fusing together it was important to keep the current as low as possible. In our measurements the current was typically $\sim$ 30 mA. The conductance was determined by measuring the voltage across a fixed resistance $R = 1.2\ \Omega$ as shown in Fig. 3. The conductance can be measured simultaneously with the pressure.

### C. Video visualization

To establish strong correlations between the motion of sand and the flow of air, coincidence measurements were carried out to visualize the sand flow on one hand and to probe the pressure fluctuations on the other. A video camera was used to image the sand flow in the vicinity of the orifice. To synchronize the measurements a short flash of light was used. The flash was registered by both the video camera and the photodiodes used for the pressure measurement. The main illumination for the sand flow was provided by a 5 mW He Ne laser. By expanding the laser beam using a lens, the structures in the sand, such as the free-fall arch and the plug, could be seen reasonably well.

## III. DISCUSSION

### A. Dynamics of the free-fall arch

The existing theoretical work on mass flow in the hour glass (see, e.g., Ref. [4]) is based on the idea of a free-fall arch which is a zone (or a boundary) separating regions where the grains are typically in contact from regions where they are typically not in contact (and thus falling). The forces acting on the particles above the free-fall arch consist of the stresses from the other particles in addition to gravity and hydrodynamic forces, whereas below the free-fall arch only gravity and hydrodynamic drag act.

The theoretical ideas of the free-fall arch and the existence of a well-defined sharp interface are rather unclear [4] and are hardly proven experimentally. As will be seen below, our experiment did indeed show a rather sharp density variation in the narrowest constriction in the sand, but it only occurred when flow in the sand was intermittent. When flow in the sand was continuous, as was the case when the hour glass was open on both ends, no sharp interface could be observed. We investigated this density front, which may be identified as the "free-fall arch," using a CCD camera. Figure 4 presents two snapshots of the interfacial configurations corresponding to before and after the formation of the plug. Light was strongly scattered from the free-falling particles in the low-density region and is seen as a bright area in Fig. 4. Since the laser beam could not penetrate into the dense regions of the sand, these regions appear dark on the picture. The sharp interface (or the arch) $I_1$ between high and low sand density is clearly seen in these photographs.

To characterize the interfacial fluctuations we measured the location of the interface $I_1$ as a function of time. Here the time resolution was 0.02 s determined by the video rate of our CCD camera. Synchronized measurements of the position of the free-fall arch and the pressure in the lower chamber are shown in Fig. 5 for hour glass A. The upper curve shows the pressure measurements and the lower curve (A) shows the position of the free-fall arch. On the same graph we also plotted the location of the upper interface of the plug, marked as $I_0$ in Fig. 4(b). This curve is denoted as (B). The interface $I_0$ appeared during the end of the active phase. In the pressure and the visualization experiments we observed two types of oscillations. One was slow and had a period typically one second [9]. The other was fast and had a period of a few tenths of a second [10], and it existed only in the active phase. The vertical position of the free-fall arch was strongly correlated with the pressure fluctuations. An increase in pressure occurs when the interface moved upward, while a decrease in the pressure was typically observed when the interface did not move or when the interface moved slightly downwards.

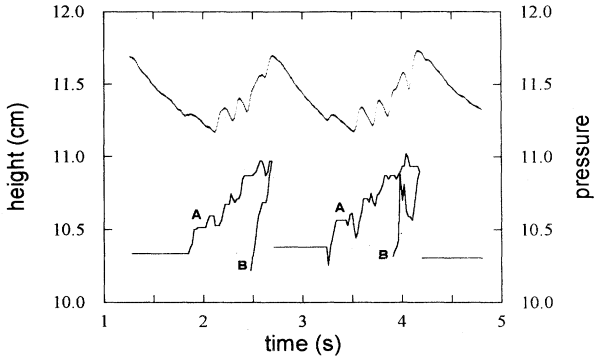


FIG. 5. The upper curve: the time dependence of the pressure fluctuations measured in hour glass A. The lower curve: the position of the arch A and the upper "interface" B of the plug as a function of time. The pressure fluctuations are shown with an arbitrary scale. The lower curve is in units of cm and is the distance from the bottom of the hour glass. The particle size in the experiment is $d = 89$ $\mu$m.

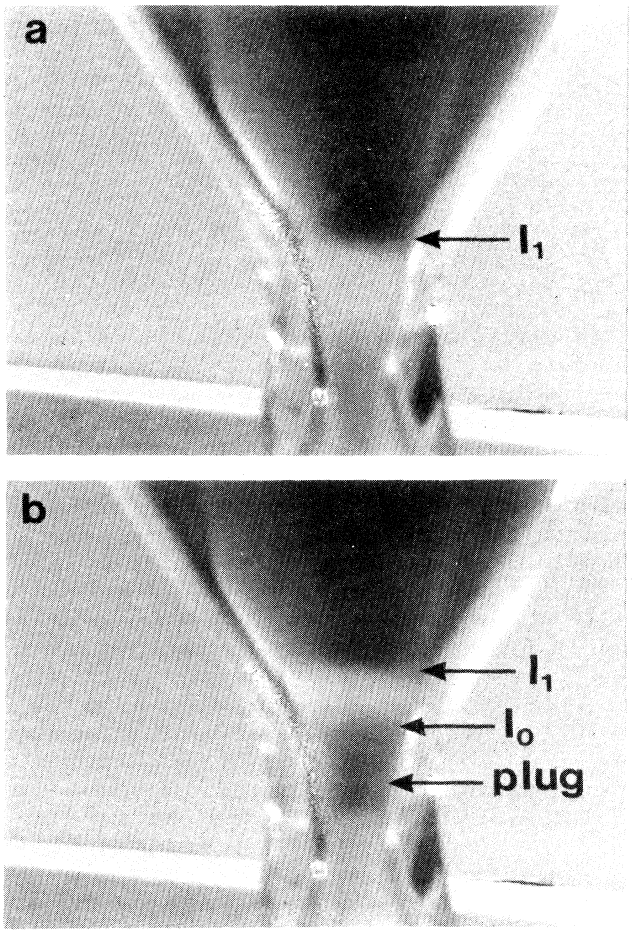


FIG. 4. Photographs of the flow in the active phase illustrating the dynamics of the free-fall arch $I_1$ and the plug formation. (a) The picture shows the "free-fall arch" $I_1$ before the formation of a plug. (b) The picture shows plug formation and the "free-fall arch" $I_1$ just after the plug formation. The upper interface of the plug is indicated by $I_0$.

In our earlier work [9] the period of the oscillations was found to be rather insensitive to the particle size. Our recent measurements with different hour glasses, however, indicate that there could be a particle-size dependence on the oscillation period, and this dependence appears to be determined by the geometry of the hour glasses. We further note that the size-dependent measurements are intrinsically difficult, particularly with small sized particles. Moisture in the air, electrostatic interactions, and the surface roughness all conspire to make the measurements unreliable for small particles.

### B. Plug formation and propagation of low-density zone

One of the interesting findings in the flow visualization experiments was the observation of plug formation in the narrowest part of the orifice. The plug was created when the flux of particles coming from the free-fall arch was too large to pass through the orifice rapidly. The accumulation of particles in the narrowest constriction severely restricted the flow of air, thus allowing the pressure gradient to build up in the orifice which further stabilized the plug. The appearance of the plug signaled the end of the active phase. Despite the absence of sand flow from the upper to the lower chamber after the formation of the plug, there was still a great deal of movement of sand above the plug. This could be characterized by the appearance of an air "bubble" which propagated upwards and eventually disappeared in the sand heap. Figure 4(b) shows a snapshot of the plug and the bubble as it traveled upwards. It is intriguing that a bubble with a reasonably sharp interface can form in a granular material considering that there is no interfacial tension between the sand and the air. The stability of the interface seen here therefore must involve hydrodynamic interactions between the grains, and the grains with the

air. The latter effect is clearly due to the differential pressure across the interface which stabilizes the sharp density stratification.

### C. Inactive phase: Darcy flow

When the sand falls from the upper into the lower chamber, the pressure increases in the lower chamber and decreases in the upper chamber. However, when the flow ends, the pressure gradient decreases due to the fact that the sand is permeable to air. The change in the pressure gradient is related to the air current passing through the sand matrix in the orifice. By using the Darcy law in the inactive regime, the pressure difference between the upper and the lower chamber can be calculated with the result [9]

$$\Delta P = \Delta P^{max} \exp(-t/\tau), \tag{1}$$

where $\Delta P^{max}$ is the maximum pressure difference between the two chambers at $t = 0$ and $\tau$ is the characteristic time given by

$$\tau = \eta V / P_0 \pi \kappa R \tag{2}$$

with $V$ being the volume of the upper chamber, $P_0$ the average pressure in the hour glass, $\eta$ the air viscosity, and $\kappa$ the permeability of the sand. In this calculation it has been assumed that the pressure difference is localized in a small region, $\sim R^3$ in the orifice. The size $R$ provides a useful length scale from which the pressure gradient can be calculated. Within our simple model, the pressure relaxes exponentially with a time constant that depends on the internal pressure of the gas $P_0$. We emphasize that the above calculation does not include the effect of sand compactification during the inactive phase. Such an effect, though nonlinear in character, has little influence on the pressure measurements. When the air pressure $\Delta P$ between the two chambers becomes smaller than a minimum pressure $\Delta P^{min}$, the sand becomes unstable and starts to flow again. The pressure fluctuations between the lower chamber and the atmospheric pressure are shown in Fig. 6 for measurements with the hour glass A filled with 89 $\mu$m particles. Note that the pressure difference $\Delta P$ between two chambers, defined earlier, is twice the pressure difference between one of the chambers and the atmospheric pressure, which is shown in the figure. Experimentally we found that $\Delta P^{max}$ and $\Delta P^{min}$ were nearly independent of particle size, and were approximately 23 and 10 mm of water, respectively. These values were reasonably constant, i.e., independent of time, for a given particle size.

In order to verify experimentally Eq. (2), we changed the average pressure $P_0$ in hour glass A by compressing air into the hour glass using a large syringe. The frequency of the slow oscillation was measured by monitoring intensity fluctuations of a He-Ne laser beam which passed through the neck of the hour glass. Since the viscosity of air is independent of pressure, the relaxation time $\tau$ should be inversely proportional to $P_0$. This was indeed seen in the experiment. Figure 7 shows the inactive time $T_i$, which is proportional to $\tau$ [9], as a function of the dimensionless pressure $P_a/P_0$, where $P_a$ is the atmospheric pressure. The data can be fit reasonably well by a line which passes through the origin. This is consistent with Eq. (2). The scattering in the data was partly due to the cohesive forces and partly due to small temperature variations between the two chambers. These effects, though small, were quite discernible in the experiment, reflecting the sensitivity of our measurements.

Usually the importance of the interstitial fluid is related to whether the intergranular forces are transmitted through direct contacts between grains or through hydrodynamic forces due to the interstitial fluid. The ratio between these forces defines the *Bagnold number* $B$. An estimate of the Bagnold number for the hour glasses used in our experiments indicates that the dominant effect of the interstitial fluid is *collective* rather than free single-particle behavior. As was shown in Ref. [9], we may estimate the ratio between the gravity and hydro-

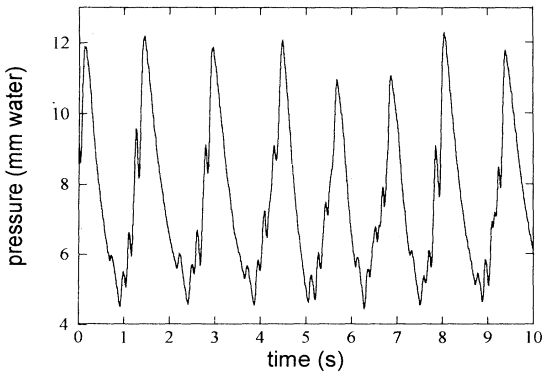


FIG. 6. Pressure fluctuations as a function of time for $d = 89$ $\mu$m particles in hour glass A with $D = 3.7$ mm. The measured pressure is the differential pressure between the lower chamber and the atmospheric pressure.

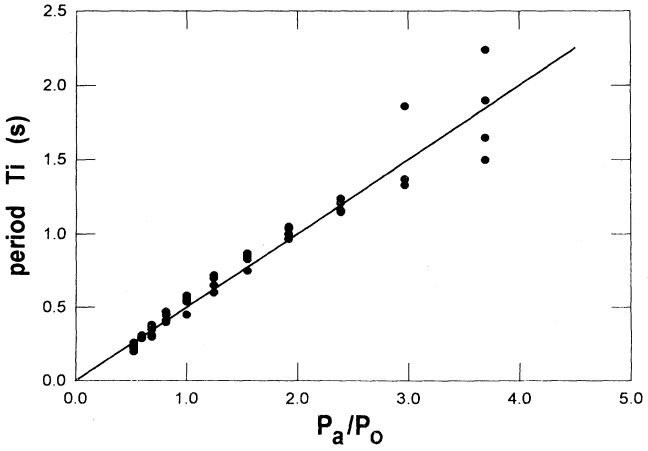


FIG. 7. The inactive time $T_i$ as a function of $P_a/P_0$, where $P_a$ is the atmospheric pressure and $P_0$ is the average pressure in the hour glass.

dynamic forces for a single grain which is not in contact with the others. Using the expression for the drag force on a spherical particle of radius $r$ moving with velocity $v$ in a Newtonian fluid of viscosity $\eta$ and density $\rho$, we find the Bagnold number to be $B = 2r^2 g\rho/9\eta v$, where $g$ is the gravitational acceleration. Using the numbers found in the intermittent regime of our hour glasses, we estimated $B$ to be approximately $10^3$. Thus, the hydrodynamic forces are not capable of competing against gravity for a single free grain. However, it is quite reasonable that when hydrodynamic interactions act on a collection of particles, the situation could be quite different. As will be seen below, the mechanism behind the blocking of the flow is the formation of a plug in the narrow constriction of the hour glass. This plug is a collective structure, and what we have to understand is the equilibration of such a structure under the influences of gravity, friction (between two grains and between grains and the wall), and hydrodynamic forces. The intermittent flow seen in the experiments strongly suggests that in reality the hydrodynamic and mechanical forces in the system are of the same magnitude. Namely, the system is operating near marginal (in)stability: Sometimes the hydrodynamic forces dominate, and sometimes the mechanical forces dominate. When the former occurs the sand stops flowing, whereas when the latter occurs the sand starts flowing. As a result, the Bagnold number is of the order of unity. Using this reasoning, we may estimate the mechanical forces using the hydrodynamic ones, which are easier to determine. The hydrodynamic forces are those induced in a porous medium by a pressure gradient across it. The pressure gradient is concentrated across a small volume $D^3$ in the vicinity of the orifice and the pressure difference $\Delta P$ between the chambers is of the order of $10 - 24$ mm water in these experiments. The contact forces we estimate to be the weight of the grains within a volume $\xi^3$, where $\xi$ is a characteristic length scale related to the size of the mesh of the network transmitting forces within the sand, and $\phi$ is volume fraction of the grains [18], for which to the lowest approximation one may use the value for random close packing of spheres. This weight constitutes the "granular pressure." It is important to note that $\xi$ in general is much smaller than the height of the sand pile. When the sand is not flowing, the granular pressure of the sand itself will balance the hydrodynamic forces, and we estimate $\xi = \Delta P/(\rho_g g\phi) \approx 8$ mm.

### D. Inactive phase: Compactification

Although the effect of compactification might be negligible for the pressure measurements, it manifested itself in the conductance measurements. Figure 8 shows the conductance (lower curve) as a function of time. For clarity the electrical conductivity measurement was carried out simultaneously with the pressure measurement, which is displayed as the upper curve in the same graph. Several features in the figure are interesting. First, unlike the pressure, the modulation in the conductance is nearly 100% with the conductance approximately saturating at 0.5 $\Omega^{-1}$ during the inactive phase, whereas it drops to nearly zero during the active phase. Second, the fast oscillations in the conductance are seen in the active phase, and they appear to be commensurate with the fast oscillations seen in the pressure curve. These oscillations may be interpreted as there being free-fall arches moving in a pulsatile fashion near the electrodes. Since the conductance is proportional to the average coordination number [17], our measurements give a qualitative assessment to the local structure of the plug. In the active phase when the sand is moving, the grains are loosely packed giving rise to an overall reduction in the conductance. In the inactive phase, on the other hand, the grains are much more closely packed giving rise to a high conductance. A close inspection of the conductance curve in the inactive phase shows that there is a gradual increase in the conductance. This suggests that as the sand grains settle into a quasistatic configuration the average number of contacts between the grains increases. A rough estimate shows that the average coordination number increases by 7% during the inactive phase.

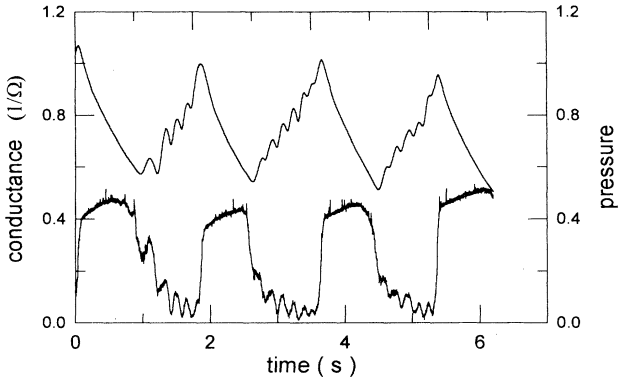


FIG. 8. The time dependence of the pressure and the conductance for beads of size $d = 89$ $\mu$m and hour glass B. The conductance is the lower curve with units $\Omega^{-1}$. The pressure is the upper curve using an arbitrary scale.

To ensure that small oscillations in both the pressure and the conductance measurements were not due to disturbances as a result of the pressure sensor, the conductance was also measured with the pressure sensor disconnected. The results shown in Fig. 8 were reproducible.

### E. Pressure measurements in the sand

Measurements of pressure fluctuations at different heights in hour glass A are shown in Fig. 9(a). In these measurements, the upper chamber was open to the atmosphere. It is interesting that the fast oscillations in the active phase were totally absent in this case. Since the local measurements require insertion of a pressure probe, which is 1 mm in diameter, the observation clearly shows ultrasensitivity of granular flow to the imposing boundaries. The presence of the probe alters the granular flow in two significant ways: (1) it limits the pathway of sand flow, and (2) it changes the stress distribution in the sand near the orifice. It is anticipated therefore that both effects can have profound influences on the formation of arches in the orifice, thus altering overall flow behavior

in our hour glass.

Despite significant disturbance to the granular flow, our measurements provided a useful diagnosis for the air pressure distribution in the hour glass, which would be otherwise difficult to obtain. Figure 9(b) is a sketch of the positions where the pressures were measured. The shaded area represents the range between the lowest and the highest position of the free-fall arch. As shown in Fig. 9(a), both the mean pressure as well as the pressure fluctuations increase as the height decreases in the orifice. On the other hand, the period of pressure variations is constant for all the heights.

In Fig. 10 the average maximum (solid dots) and minimum (open dots) pressures are plotted as a function of height. From the flow visualization experiment it was found that the maximum pressure corresponds to the moment just before the inactive period starts. It was also observed that a small number of sand grains fell from the lower part of the orifice just when it became stabilized, i.e., at the very end of the active phase. Therefore, the position of the lower sand surface just before stabilization was lower than the position just after stabilization. This can be seen as a decrease in the maximum pressure curve for the height interval between 10.0 cm and 10.5 cm. This decrease is not seen in the average minimum pressure curve because there is no sand in that part of the tube giving rise to a pressure gradient. Another interesting observation is the different slopes in the maximum and the minimum curves for heights in the region of the shaded part of Fig. 9(b), indicated by the two vertical lines in Fig. 10. This difference in the slope is consistent with the compactification of the sand which was also observed in the conductance measurements described above.

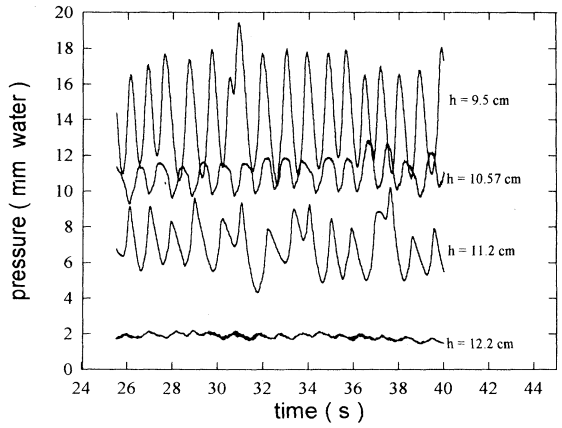


FIG. 9. (a) Pressure measurements as a function of time at different positions $h$ along the central vertical axis of hour glass A. (b) The drawing represents the neck of the hour glass with indications on the locations where the pressure measurements were performed. The values on the right-hand side represent the heights where the pressure measurements have been performed. The values on the left side are the narrowest part of the orifice, $h = 10.25$ cm, the lowest position of the free fall arch, $h = 10.5$ cm, and the highest position of the free fall arch, $h = 11.0$ cm.

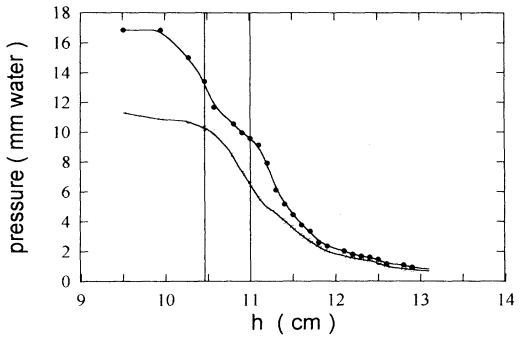


FIG. 10. The average maximum and the average minimum pressure as a function of position $h$ in hour glass A. The data of the average maximum pressure are shown with filled circles, and the average minimum pressure with open circles. The vertical lines represent the lowest and the highest position of the free-fall arch.

Simultaneous pressure measurements in both the upper and the lower chambers were performed to check if there existed a measurable phase shift between the pressure oscillations in the two chambers. To the best of our effort, no such delay was detectable. This was consistent with our visual observation, which showed synchronous motion of sand at the top of the heap and in the orifice. The observation suggests that the central region, which is most active in the mass transport and has the shape of a funnel, moves without any apparent change in the density of the sand.

## IV. CONCLUSION

The aim of this research has been to investigate the intermittent flow in hour glasses with an emphasis on the influence of the local granular structure and dynamics on the global flow behavior. We have investigated this intermittent flow behavior using different experimental techniques such as pressure, electrical conductivity, and video imaging methods. In some cases coincidence measurements with different techniques were carried out.

The experiment has largely confirmed our early physical picture that the intermittent flow is a result of delicate coupling between flow of sand and the interstitial air [9]. It is interesting that minute pressure fluctuations in the hour glass, of the order of $10^{-3}$ atm, can momentarily stop mass flow of grains completely, thus producing nearly periodic motions in the sand. The flow dynamics in the intermittent regime can be characterized by two different time scales. In the inactive phase the sand stops moving with a duration $T_i$ and in the active phase the sand moves nearly continuously with a duration $T_a$. The period of the oscillation $T(\equiv T_i + T_a)$ shows a weak, yet

observable dependence on the size of the particles used, contrary to our early findings [9]. In addition we also observed a stepwise upward movement of the free-fall arch during the active phase. This pulsatile motion has a time scale shorter than the period $T$, and the movement of the front is strongly correlated with the pressure fluctuations in the lower chamber.

In the active phase, a cluster or a plug is formed in the narrowest part of the orifice, below the free-fall arch. This plug stabilizes at the very end of the active phase and results in a "bubble" propagating in the upward direction. The pressure gradient caused by the flux of sand from the upper to the lower chamber tends to stabilize the plug, and then stops the mass flow completely creating a new stable interface.

In the inactive phase, a flow of gas from the lower to the upper chamber will decrease the pressure gradient. The pressure gradient will decrease until the sand again becomes unstable and starts to flow. The pressure in the inactive phase was measured and found to be consistent with the theoretical predictions reported by Wu *et al.* [9]. However, an additional effect was observed from synchronized conductance and pressure measurements. In the conductance measurements we observed a slight increase in the conductance during the inactive phase indicating a compactification of the sand. Independent pressure measurements internally in the sand at different heights support the idea of a local trapping of air in the sand followed by compactification.

## ACKNOWLEDGMENTS

This work has been supported in part by the CNRS and the NFR through a *Projet Internationale de Coopération Scientifique* grant. Further financial assistance was provided by the NFR, the Nansen Fund, and an EU Human Capital and Mobility grant. One of the authors (X.L.W.) acknowledges support from the NSF under Grant No. DMR 9424355.

[1] H.M. Jaeger and S.R. Nagel, Science **255**, 1523 (1992).
[2] *Disorder and Granular Media*, edited by D. Bideau and A. Hansen (Elsevier, Amsterdam, 1993).
[3] *Granular Matter*, edited by A. Metha (Springer Verlag, Heidelberg, 1993).
[4] R.M. Nedderman, *Statics and Kinematics of Granular Materials* (Cambridge Univ. Press, Cambridge, 1991).
[5] R.A. Bagnold, *The Physics of Blown Sand and Desert Dunes* (Methuen, London, 1941); R.A. Bagnold, Proc. R. Soc. London Ser. A **225**, 49 (1954).
[6] W.W. Mullins, J. Appl. Phys. **43**, 665 (1972); Powder Technol. **23**, 115 (1979); **9**, 29 (1974); J. Appl. Mech. **41**, 867 (1974).
[7] W.N. Sullivan, Ph.D. thesis, California Institute of Technology (1972).
[8] W. Bruff and A.W Jenkine, Powder Technol. **1**, 252 (1967).
[9] X-l. Wu, K.J. Måløy, A. Hansen, M. Ammi, and D. Bideau, Phys. Rev. Lett. **71**, 1363 (1993).
[10] K.J. Måløy, M. Ammi, D. Bideau, A. Hansen, and X-l. Wu, C. R. Acad. Sci. Paris **319**, 1463 (1994); D. Bideau, F.X. Riguidel, A. Hansen, G. Ristow, X-l. Wu, and K.J. Måløy, in *Non-Linearity and Breakdown in Soft Condensed Matter,* edited by K.K. Bardhan, B.K. Chakrabarti, and A. Hansen, Springer Lecture Notes Vol. 437 (Springer, Berlin, 1994).
[11] E. Manger, T. Solberg, and B.H. Hjertager (unpublished).
[12] G.W. Baxter, R.P. Behringer, T. Fagert, and G.A. Johnson, Phys. Rev. Lett. **62**, 2825 (1989).
[13] K.L. Schick and A.A. Verveen, Nature **251**, 599 (1974).
[14] A.W. Jenike, Mech. Engineering **May**, 41 (1964).
[15] C.A. James, T.A. Yates, M.E.R Walford, and D.F. Gibbs, Phys. Educ. **28**, 117 (1993).
[16] J.P. Bouchaud, M.E. Cates, and P. Claudin, J. Phys. (France) I **5**, 639 (1995).
[17] See, e.g., Chap. 4 of *Statistical Models for the Fracture of Disordered Media,* edited by H.J. Herrmann and S. Roux (Elsevier, Amsterdam, 1990).
[18] See, e.g., Chap 8 of *Disorder and Granular Media,* edited by D. Bideau and A. Hansen (Elsevier, Amsterdam, 1993).

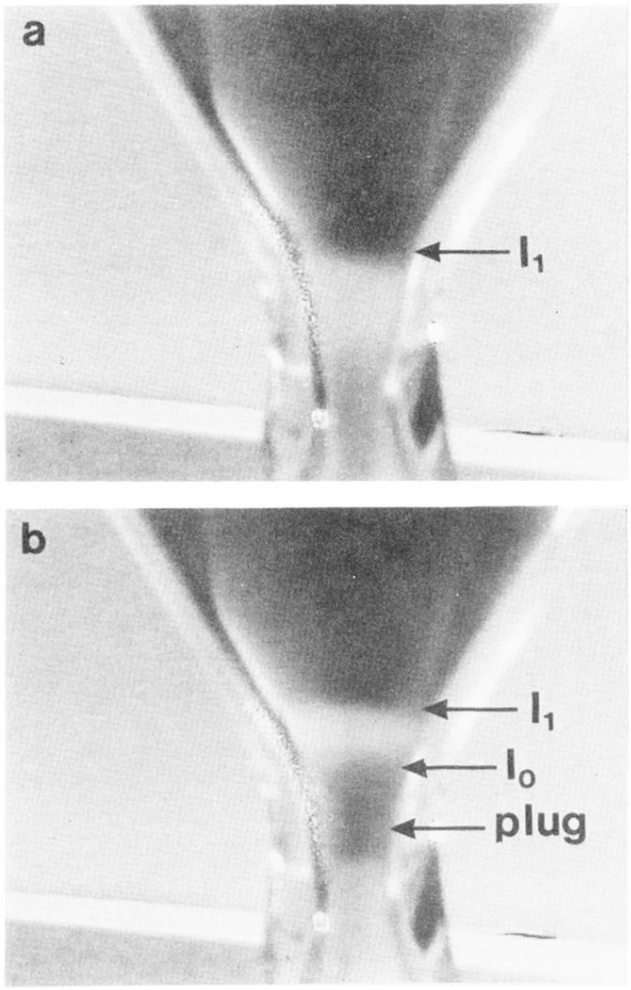


FIG. 4. Photographs of the flow in the active phase illustrating the dynamics of the free-fall arch $I_1$ and the plug formation. (a) The picture shows the "free-fall arch" $I_1$ before the formation of a plug. (b) The picture shows plug formation and the "free-fall arch" $I_1$ just after the plug formation. The upper interface of the plug is indicated by $I_0$.